

EXPERIMENTAL AND COMPUTER SIMULATION  
ANALYSIS OF A GUNN DIODE

Y. Ito, H. Komizo, T. Meguro,  
Y. Daido, and I. Umebu

Fujitsu Laboratories Ltd., Kawasaki, Japan

Summary

Bias voltage-and frequency-dependencies of dynamic admittance of a Gunn diode have been measured systematically in the 8 to 13GHz frequency range. We qualitatively verified the results by computer simulation.

Introduction

In this presentation, we describe large signal electronic admittance of a Gunn diode, measured in a coaxial mount at various operating bias voltages beyond threshold voltage.

This presentation shows that measured electronic admittance very nearly coincided with calculated values through computer simulation. This information is very useful in solving oscillator circuit design problems.

Electronic Admittance Measurement

Fig. 1(a) shows a coaxial mount which permitted precise admittance measurement over a wide frequency range, from 8 to 13GHz. We placed a Fujitsu Gunn diode (shown in Fig. 1(b)) at the end of the coaxial line ( $Z_0=50\Omega$ ). Its carrier concentration is about  $1.5 \times 10^{16} \text{ cm}^{-3}$ , the active layer is about  $10\mu\text{m}$  thick, and the threshold voltage is about 3.0 volts. At operating bias voltages of 5.5, 7.0, and 8.9 volts, oscillating frequency and output power are adjusted by sliding the metal rings. After adjustment, we measured load admittance  $Y_L$  from the diode electrode as the reference plane (T-plane in Fig. 2(a)).

Dynamic electronic admittance  $\bar{Y}_e$  ( $=-\bar{G}+j\bar{B}$ ) can be calculated by subtracting parasitic admittance of the packaged diode from  $-Y_L$ .

Figs. 2(a) and (b) show the schematic diagram of the coaxial mount and its equivalent circuit proposed by W. J. Getsinger<sup>1</sup>, with measured and calculated parasitic element values. In this case, series resistance of Gunn diode is included in  $\bar{Y}_e$ .

Results of Experiment

Figs. 3(a), (b) and (c) show measured  $\bar{Y}_e$  for each voltage as a frequency parameter. The figures show output power delivered to the load in mW. From the figures, we can clearly distinguish the following Gunn diode characteristics.

- 1) Admittance slope  $\partial\bar{B}/\partial\bar{G}$  changes clockwise from negative to positive as frequency increases.
- 2) At constant frequency and bias voltage, output power tends to increase as  $|\bar{G}|$  increases.
- 3) At constant bias voltage, maximum output power is reached slightly below the transit-time frequency (10GHz) and output power drops sharply in quenched mode operation frequency.
- 4) At a higher than 7.0 bias voltage,  $\bar{B}$  increases as bias voltage increases. This means that the diode used has a negative slope at the oscillating frequency with respect to bias voltage. A similar relationship holds for temperature.

Computer Simulation

We performed simulation, using a FACOM-230-60, applied to a one dimensional model; length  $L$  of  $10\mu\text{m}$ , uniform active layer (donor density of  $2 \times 10^{15} \text{ cm}^{-3}$ ) and suitable analytical  $v_A$ -E curve<sup>2</sup>. Fig. 3(d) shows calculated normalized electronic admittance with cross-sectional area of  $2 \times 10^4 (\mu\text{m})^2$ , when bias voltage is 8.9 volts and frequencies are 8, 10 and 12GHz, respectively. Results were highly consistent with measured values in many respects.

Application to Circuit Design

Fig. 4 shows load admittance ranges, graphically calculated using equations developed by K. Kurokawa<sup>3</sup>, for stable free-running and injection-locked oscillations. Points  $a_1, a_2, a_3$  represent the intersecting points of load admittance  $Y_L(\omega)$  and electronic admittance  $-\bar{Y}_e$  (shown in Fig. 3(a)) for free-running oscillating frequencies of 8.4, 10.0 and 13.4GHz, respectively. The solid line AB is the tangent of  $-\bar{Y}_e$  curve at each intersecting point.

Free-running oscillation is stable only when the vector  $Y_L(\omega)$  (frequency derivative of  $Y_L(\omega)$ ) is outside the hatched areas. And, for example, the stable range of injection-locked oscillation at 10GHz is further limited by line  $a_2C$ . If load admittance locus  $Y_L(\omega)$  (measured in an experimental injection-locked oscillator) intersects  $-\bar{Y}_e$ , as shown in the figure, the locking frequency range becomes unsymmetrical for upper and lower locking signal frequencies from the free-running frequency (i.e. the upper locking range is wider than the lower). Furthermore, output power decreases as locking

signal frequency increases, within the locking range. These phenomena can be clearly deduced from the following facts: The  $-\bar{Y}_D$  line changes clockwise as frequency increases and output power increases inversely to RF amplitude on the G-B curve.

The measured external Q of this oscillator was about 13 at a locking gain of 10dB and output power deviation was within 0.5dB over the full locking range. We applied further careful design to MIC injection-locked oscillator and obtained an extremely low external Q of 4, output deviation of 1.5dB, output power greater than 21.8dBm.

### Conclusion

We measured in detail the bias voltage- and frequency-dependence of dynamic electronic admittance of a Gunn diode and qualitatively verified our results through computer simulation.

We have provided, as an example, graphical circuit design of a broadband injection-locked oscillator.

### References

- 1) W. J. Getsinger, "The Packaged and Mounted Diode as a Microwave Circuit," IEEE Trans. MTT, Vol. MTT-14, No. 2, pp. 58-69, Feb. 1966.
- 2) H. W. Thim, "Computer Study of Bulk

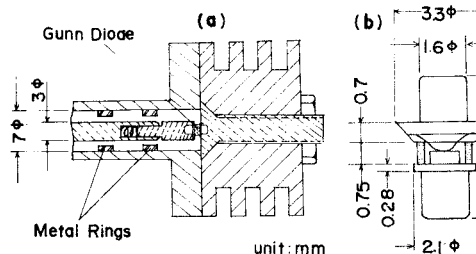


Fig. 1(a) Cross sectional view of the coaxial mount  
(b) Packaged diode dimensions

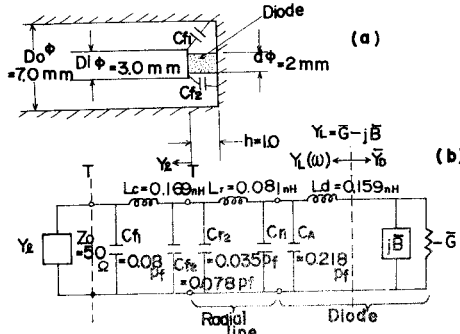


Fig. 2(a) Schematic diagram of the coaxial mount  
(b) Its equivalent circuit looking from T-plane

GaAs Devices with Random One-Dimensional Doping Fluctuations," Journal of Applied Physics, Vol. 39, No. 8, pp. 3897-3904, July 1968.

- 3) K. Kurokawa, "Some Basic Characteristics of Broadband Negative Resistance Oscillator Circuits," Bell Sys. Tech. J., Vol. 48, No. 6, pp. 1937-1955, July-August 1969.

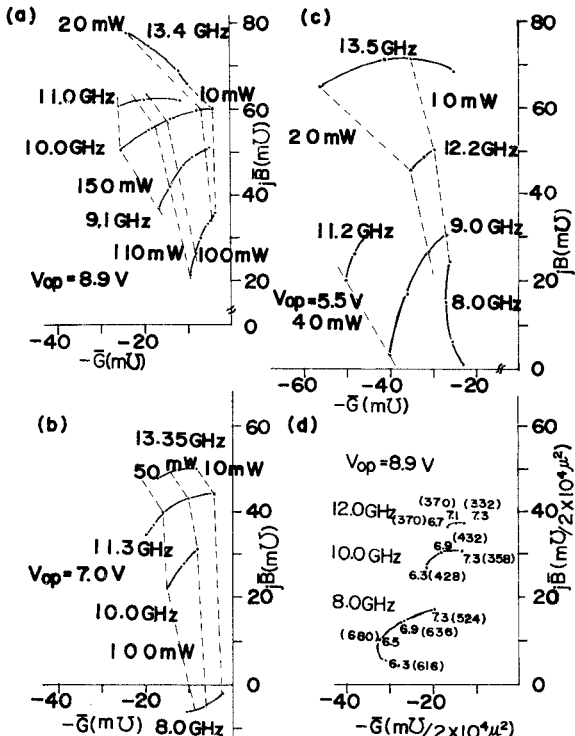


Fig. 3(a)-(c) Measured electronic admittance. Solid lines indicate  $\bar{Y}_D$ .  
(d) Calculated electronic admittance. Figures represent RF voltages and figures in parentheses output power in mW.

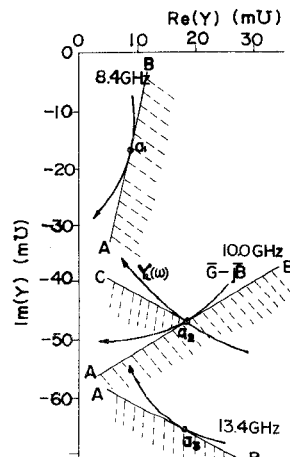


Fig. 4  
Stable range of load admittance  $Y_L(w)$  for free-running and injection-locked oscillation, using electronic admittance  $\bar{Y}_D$  shown in Fig. 3(a)